4.5.1. EARTHQUAKE GROUND MOTION SCENARIOS IN URBAN AREAS: THE CASE OF THE CITY OF THESSALONIKI (NORTHERN GREECE)

Z. Roumelioti, A. Kiratzi, N. Theodulidis, A. Panou, A. Savvaidis, C. Benetatos

4.5.1.1. Introduction

On June 20, 1978, Thessaloniki, the largest and most densely populated city in Northern Greece, experienced the devastating consequences of an M_w=6.4 earthquake, whose epicenter was located about 30 km east-northeast from the centre of the city. This earthquake, herewith referred to as the "Stivos earthquake", was the first one to hit a modern Greek city and therefore alerted public authorities and the local scientific community about the necessity of increasing the preparedness against such catastrophic events. As a consequence, since 1978 a large number of studies has been conducted on the characteristics of the last catastrophic earthquake, the regional tectonics and other elements contributing to the overall seismic risk in the broader area of the metropolitan city of Thessaloniki. For an extended list of relative publications the reader is referred to the recent works of Stiros and Drakos (2000), Tranos et al. (2003), Theodulidis et al. (2005) and Roumelioti et al., (2005) and the references therein.

Nowadays, the most challenging target for seismologists and earthquake engineers is the incorporation of the gained knowledge on the seismotectonics of the area and the geotechnical characteristics of the geological formations of Thessaloniki, into realistic earthquake scenarios that could contribute to effective planning for and mitigation of earthquake hazard in the wider metropolitan area. Simulation of strong ground motion from scenario earthquakes provides a perspective on the plausible levels of ground shaking within the area of interest and subsequently on the seismic impact and helps public authorities, emergency responders and scientists to better design and coordinate an emergency plan for a future earthquake.

Towards this direction, we present the simulation results for a scenario earthquake of M_w=6.2 in the proximity of Thessaloniki. Simulations have been performed using the finite-fault simulation code FINSIM (Beresnev, Atkinson, 1998). The applicability of the code to ground motion predictions has been tested and verified by numerous researchers and in various seismotectonic environments (e.g. Hartzell et al., 1999, Castro et al. 2001, Beresnev, Atkinson 2002, Hough et al. 2002, Roumelioti, Kiratzi, 2002). This code and the stochastic method in general, have also been previously applied in Greece to simulate strong ground motions from past strong earthquakes (Papastamatiou et al., 1993, Margaris, Papazachos, 1994, Margaris, Boore, 1998, Roumelioti et al., 2000, Roumelioti et al., 2003, Benetatos, Kiratzi, 2004, Roumelioti et al., 2004). Recently, Theodulidis et al. (2005) applied the stochastic method to simulate the strong ground motion from the 1978 Stivos earthquake, within the municipal area of Thessaloniki. The results of the aforementioned study were compared to macroseismic data and one strong motion waveform (recorded at the centre of

Thessaloniki) of the 1978 earthquake and the agreement between synthetic and observations was found to be quite satisfactory. The study of Theodulidis et al. (2005) consists the basis for our simulations, as we employ the same, already validated in the area of Thessaloniki, modelling parameters for the path and site effects.

4.5.1.2. Regional Seismotectonic Setting

Thessaloniki lies in the northern part of the Aegean Sea region (Fig. 4.5.1.1), where seismotectonics are controlled by the N-S extension of the back-arc area and the dextral strike-slip motions transferred from the east, along the western termination of the North Anatolian Fault Zone (NAFZ), into the Aegean (Kiratzi, 2002). The geologic basement of the broader area consists of pre-alpine and alpine rocks, which carry the imprints of the homonym deformation in the form of thrust, reverse and strike-slip faults, whereas normal and oblique-slip faults have also been formed or reactivated by the post-orogenic extension. These latter structures have created basins of different orientations, which have been filled with Neogene and Quaternary sediments. The orientations of the post-orogenic basins vary from NNE-SSW to E-W, although the predominant orientation is NW-SE. The E-W trending predominant orientation is NW-SE. The E-W trending faults are few and rather small, but presently active as they are oriented perpendicular to the active stress regime.

One of the quaternary basins, which is of primary importance for the seismic hazard of the wider area of Thessaloniki is the so-called Mygdonian graben located to the east-northeast of the metropolitan area (Figs. 4.5.1.1 and 4.5.1.2). This graben is associated with historical and recent earthquakes which had impact on the built environment of the city (Papazachos, Papazachou, 2003), among which the recent catastrophic event of 1978. The basin was formed during lower Miocene within the crystalline mass of the Servomacedonian geological zone and was subsequently filled with Neogene and Quaternary sediments. The geological history of the graben is associated with NW- and NE-trending strike-slip or oblique normal faults, the most important of which seem to mark the SW margins of the graben, along the coast of the Langadha Lake (Mercier et al., 1983, Pavlides, Kilias, 1987). Many researchers, who studied the 1978 earthquake sequence, identify the southwestern faults of the Mygdonian graben as the continuation of the 1978 seismogenic fault to the west. However, in a recent work, Tranos et al. (2003) suggested that the western continuation of the 1978 rupture zone is located more to the south, outside the Mygdonian graben and consists a severe threat for the city of Thessaloniki.

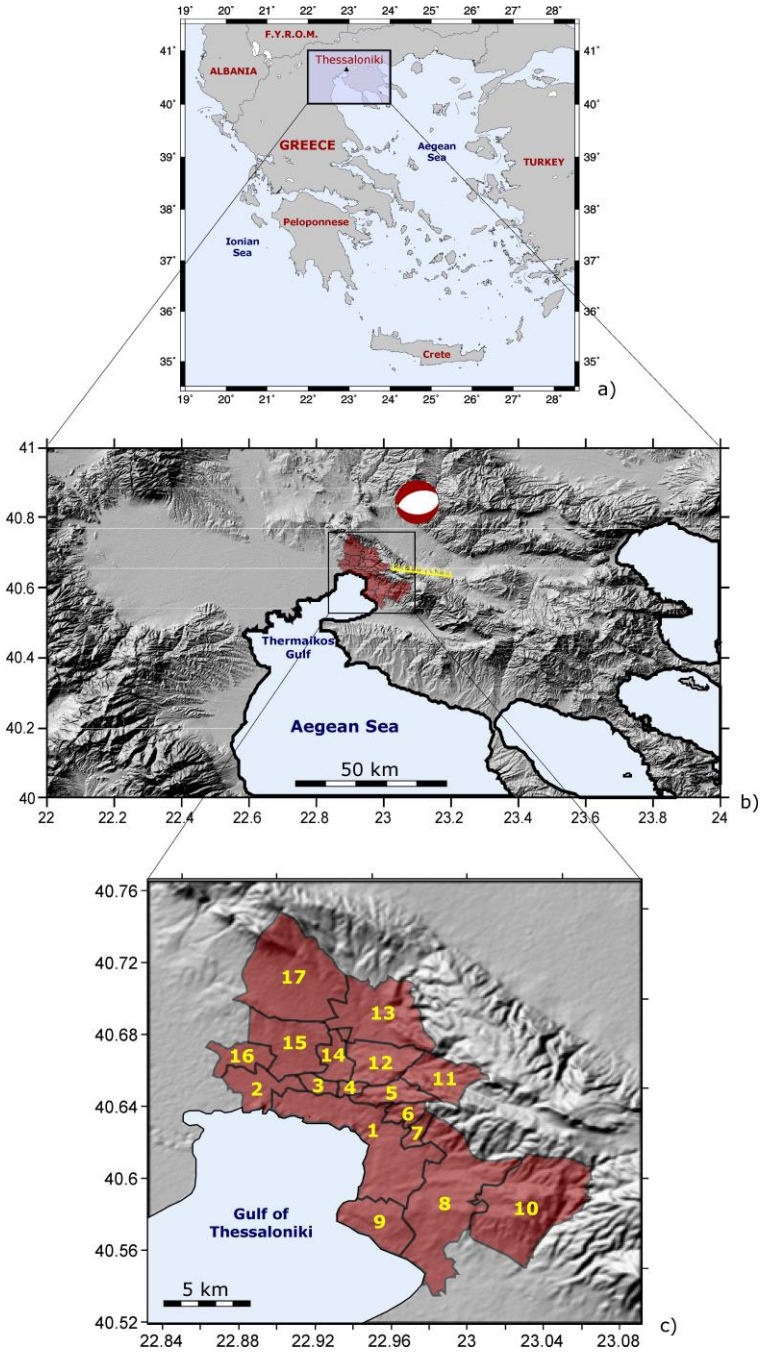

Fig. 4.5.1.1. (a) Map showing the location of the wider study area; (b) location of the fault model (thick toothed line on the downthrown side) and adopted focal mechanism of the M_w=6.2 scenario earthquake. The frame sets the boundaries of the area within which we have performed stochastic simulations of strong ground motion (c) the metropolitan area of Thessaloniki with its municipalities:

1: Thessaloniki; 2: Menemeni; 3: Ampelokipi; 4: Neapoli; 5: Sikies; 6:Ag. Pavlos; 7:Triandria; 8:Pylaea; 9:Kalamaria; 10:Panorama; 11:Pefka; 12:Polichni; 13:Efkarpia; 14:Stavroupoli; 15:Evosmos; 16:Eleftherio-Kordelio; 17:Oreokastro.

4.5.1.3. Scenario earthquake

The selection of the scenario earthquake was based on the recent work of Tranos et al. (2003) about the western extension of the 1978 Stivos earthquake fault zone. According to this study, the 1978 fault zone continues to the west, towards the city of Thessaloniki, in the form of a large number of sub parallel fractures and faults, which consist the so-called Thessaloniki – Gerakarou Fault zone (Fig. 4.5.1.2). This zone starts at the village of Gerakarou, where the 1978 surface ruptures terminated (Papazachos et al., 1979), passes through or next to the villages of Chortiatis, Exohi, Asvestochori and ends close to the village of Pefka, within the municipal area of Thessaloniki. The eastern and central parts of the zone present an east-west orientation similar to the one inferred by the focal mechanism of the 1978 earthquake, whereas its western part bends more to the northwest. The entire zone dips to the north.

Tranos et al. (2003) studied the Coulomb stress changes caused by past earthquakes within the Mygdonian graben and concluded that, due to the 1978 earthquake, the Thessaloniki – Gerakarou fault zone has been brought closer to failure and therefore consists a severe threat for the population and the built environment of Thessaloniki. This result triggered us to study the distribution of strong ground motion from a scenario earthquake at the Thessaloniki – Gerakarou fault zone, the goal being the assessment of the ground motion level throughout the city of Thessaloniki and the recognition of municipal areas that would most probably experience the strongest shaking.

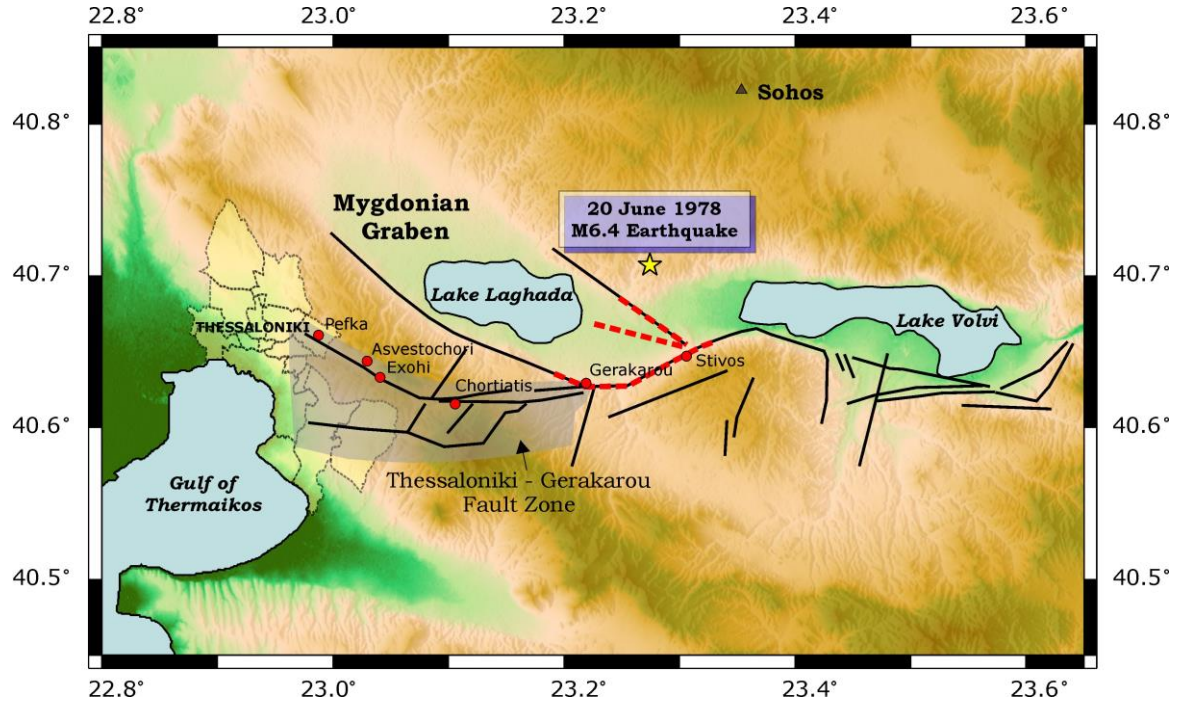

Fig. 4.5.1.2. Regional map showing the proposed by Tranos et al. (2003) faults along the southern margin of the Mygdonian graben (black lines). The Thessaloniki – Gerakarou fault zone (as defined by Tranos et al., 2003) is included in the grey polygon. The surface ruptures (red discontinuous lines) and the epicenter (star symbol) of the 1978 earthquake (Papazachos et al., 1979) are also shown

For our scenario earthquake we assume the rupture of the eastern and central parts of the Thessaloniki – Gerakarou fault zone, and more specifically the part from Gerakarou to Exohi villages. Between Exohi and Asvestochori villages, Tranos et al. (2003) identified a minor fault bend, which could act as a barrier in a future activation of the Thessaloniki-Gerakarou fault zone. Taking also into account the change of orientation between the parts eastwards and westwards of Exohi village, we consider as more probable scenario that the two parts would not rupture during one single event.

Consequently, the assumed rupture length is of the order of 15 km. Using the empirical relations of Wells and Coppersmith (1994) and Papazachos et al. (2004), a rupture length of this order corresponds to an earthquake of M_w=6.2, a value which was adopted for our scenario earthquake.

4.5.1.4. Stochastic Simulation

The method used to assess the expected strong ground motion from the scenario earthquake is the stochastic method for finite sources, which is based on the idea that high-frequency motions can be considered random (Hanks 1979, McGuire and Hanks 1980, Hanks and McGuire 1981). Boore (1983) was the first who applied this idea to simulate strong ground motions from point sources and few years later Beresnev and Atkinson (1997) extended the original method to encompass effects from finite sources. The method of Beresnev and Atkinson (1997) involves discretization of the fault plane of the simulated earthquake into smaller subfaults, each of which is assigned an ω^2 spectrum. Contributions from all subfaults are empirically attenuated to the observation site and appropriately summed to produce the synthetic accelerogram. For a detailed description of the stochastic method, the reader is referred to Boore (2003) and to references therein.

The applied method requires a simple representation of all factors affecting strong ground motion. The seismogenic source is represented by a rectangular plane, while the propagation model (geometric spreading, inelastic attenuation, near-surface attenuation and site amplification) is described by empirical relations and factors. Whereas the representation of the source is different for each scenario earthquake, the propagation model can be considered the same, assuming the same seismogenic volume and observation sites. In the case of the wider Thessaloniki area, the stochastic method has been previously applied by Theodulidis et al. (2005) to simulate strong ground motion from the 1978 earthquake. Their synthetic results were compared to macroseismic and strong motion observations with a satisfactory agreement, providing a validated set of parameters for the description of the propagation path model between the Mygdonian graben and the city of Thessaloniki. The validated stochastic parameters of Theodulidis et al. (2005) were also adopted in this study. A summary of the simulation parameters is presented in Table 4.5.1.1.

Fig. 4.5.1.3 gives a schematic representation of the adopted normal fault model of the scenario earthquake. The along-strike dimension of the fault model was measured from the map of Tranos et al. (2003) to be equal to 15 km, while the along-dip dimension was computed from empirical relations to be 11 km (Wells and Coppersmith, 1994; Papazachos et al., 2004). Based on the empirical relation $\log\Delta l = -2+0.4M$ (Beresnev, Atkinson, 1999), the fault plane was divided in 5x4 subfaults along length and width, respectively.

To cover multiple rupture scenarios, we tested different rupture initiation points by successively assigning the hypocenter position to different subfault of the fault model

area. In total, nine rupture-initiation points were considered, covering the lower ¾ of the fault area. The tested rupture initiation points are marked as asterisks in Fig. 4.5.1.3 Finally, to incorporate the uncertainty due to the lack of information about the slip distribution during a future earthquake, we examined 30 random slip distributions. Therefore, synthetic strong motion parameter values presented in this study correspond to the mean values of the results of 30×9 (random slip distribution scenarios × tested rupture initiation points) simulations.

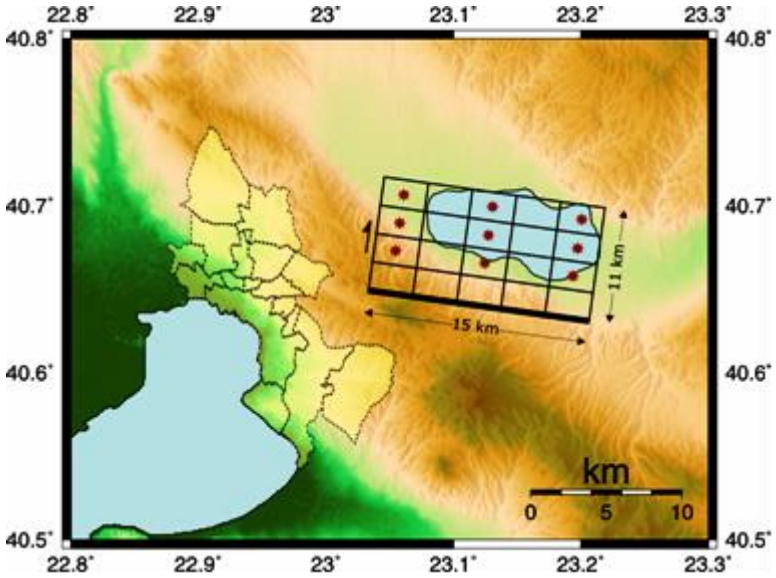

Fig. 4.5.1.3. Projection of the adopted fault model (descritized into 5×4 subfaults) for the scenario earthquake on the ground surface. Asterisks denote the locations of the different rupture initiation points adopted in the inversions

Table 4.5.1.1. Modelling parameters used to stochastically simulate strong ground motion from a scenario earthquake of M_w=6.2 at the western extension (Gerakarou – Exohi) of the 1978 fault.

Parameter	Symbol	Value
Fault Orientation	φ_1 δ_1	Strike 278° (Soufleris, Stewart, 1981) Dip 46° (Soufleris, Stewart, 1981)
Fault Dimensions	L w	Length 15 km (Tranos et al., 2003) Width 11 km (Wells, Coppersmith, 1994)
Fault Origin	alat1 alon1	40.631N (Tranos et al., 2003) 23.208E (Tranos et al., 2003)
Depth to upper edge of the fault	h	0.0 km
Mainshock moment magnitude	M_w	6.2 (Wells, Coppersmith, 1994)
Stress drop	stress	50 bars (Kanamori, Anderson, 1975)
Number of subfaults along strike and dip	$N_L \times N_W$	5×4 (Beresnev, Atkinson, 1999)
Hypocenter location on the fault	i_0, j_0	9 trial positions (1,2 – 1,3 – 1,4 – 3,2 – 3,3 – 3,4 – 5,2 – 5,3 – 5,4)
Crustal shear wave velocity	beta	3.4 km/sec
Crustal density	rho	2.72 gr/cm^3

Parameter controlling high-frequency level	**sfact**	**1.5 (Beresnev, Atkinson, 2001a,b)**
Parameter κ	**kappa**	**0.035 (Margaris, Boore, 1998)**
Parameters of the attenuation model $Q(f)=Q_0*f**eta$	**Q_0** **eta**	**100.0** **0.8 (Hatzidimitriou, 1993, 1995)**
Geometric spreading	**igeom**	**Q (1/R model)**
Distance-dependent duration (sec)		**equal to source duration (τ)**
Site effect	**namp1**	**NEHRP (1994) site amplification factors**
Slip distribution model	**islip**	**30 random models**

The realistic character of ground motion maps depends greatly upon the credibility of the depiction of site effects within the area of interest. In applications like the one presented herein, which aim at computing spatial variations of strong ground motion levels and not site-specific values, a simplified geotechnical zonation in site classes introduced in building codes is usually adequate. The geotechnical zonation of the city of Thessaloniki, adopted in this study, is based on a combination of results from previous studies of Anastasiadis et al. (2001) and Theodulidis et al. (2005). Anastasiadis et al. (2001) assembled a sufficient geotechnical database and following NEHRP (1994), deduced three soil type categories for the wider city center: rock (Site Class B, V_{S30}>750m/sec), stiff soil (Site Class C, 360m/sec<V_{S30}<750m/sec) and soft soil (Site Class D, 180m/sec<V_{S30}<360m/sec). Theodulidis et al. (2005) extended the pre-existing zonation of Anastasiadis et al. (2001) to include peripheral municipalities, based on available geotechnical and borehole data, as well as on ambient noise measurements conducted in the frame of the SEISIMPACT-THESS project (www.seis-impact.gr). Fig. 4.5.1.4 shows the simplified geotechnical zonation of Thessaloniki, according to NEHRP provisions, adopted in this study.

The current application of the stochastic method included two steps. First, simulations were performed for all points of the grid, covering the area shown in Fig. 4.5.1.1.b, c (from 40.52^{o}N to 40.77^{o}N and from 22.83^{o}E to 23.09^{o}E with a grid spacing 0.5×0.5 km). As previously mentioned, for each grid point we computed 270 synthetic acceleration time histories corresponding to equal number of different combinations of the location of the rupture initiation point and the slip distribution model. These values were then used to derive average values, which were finally used to produce smoothed strong ground motion maps (e.g. Fig. 4.5.1.5). In this stage, for each grid point we computed synthetic accelerograms for all three soil classes (B, C and D). In the second step, each grid point was assigned a site class (B, C or D), based on the geotechnical map of Fig. 4.5.1.4. Depending on the site characterization, the appropriate synthetic waveform was selected and the associated strong ground motion parameters were extracted to be used in the production of the final strong ground motion maps, which include the site effect.

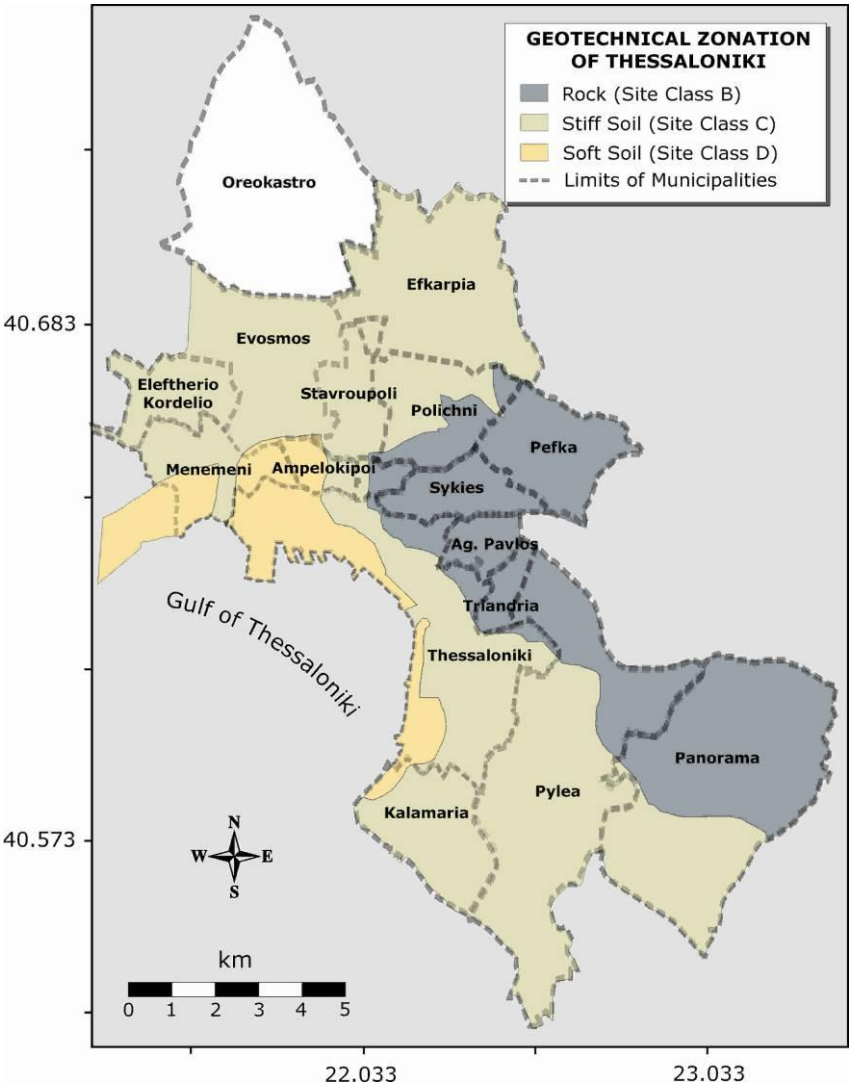

Fig. 4.5.1.4. Simplified geotechnical zonation map of Thessaloniki (combined results from Anastasiadis et al., 2001 and Theodulidis et al., 2005)

In Fig. 4.5.1.6 we present the synthetic PGA map, which includes the site effect computed by the amplification factors of NEHRP (1994), on the basis of the simplified geotechnical zonation of Fig. 4.5.1.4. Geotechnical information is not available for the entire initial grid of simulations and therefore Fig. 4.5.1.6 (and Fig. 4.5.1.7 presented later) include only those grid points that lie within the limits of the municipal area of Thessaloniki (with the exception of the municipality of Oreokastro – Figs 4.5.1.1. and 4.5.1.4. – which lies outside the geotechnically characterized area). PGA values in the map of Fig. 4.5.1.6. vary from ~0.32g in the eastern municipalities of Thessaloniki to ~0.13g within its westernmost municipalities. PGA distribution appears to be controlled mostly by the source-to-site distance, as in general, values decrease from east to west as in Fig. 4.5.1.5., which does not include any site effect. An exception to this general pattern is the coastal zone of the central part of the city, where we observed increased levels of strong ground motion due to the coverage of the specific zone by soft soil.

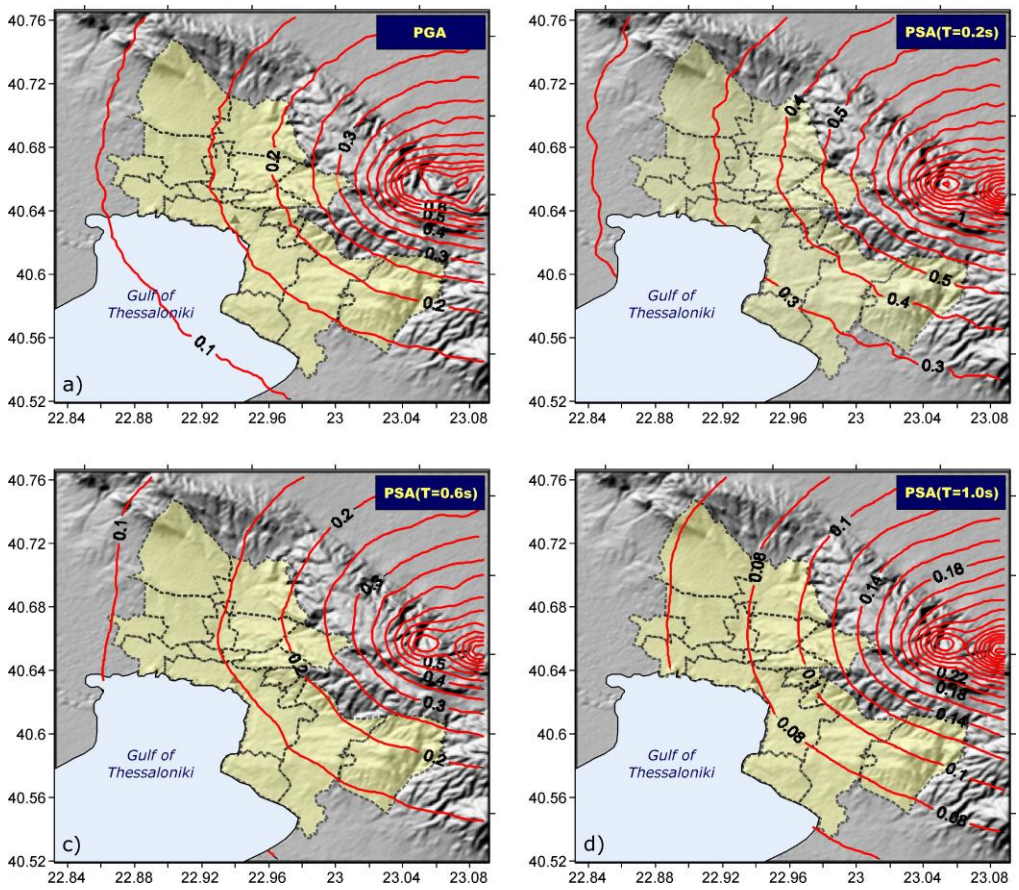

Fig. 4.5.1.5. Stochastic strong ground motion maps for the selected scenario earthquake prior to the incorporation of site effects (all simulations are for Site Class B): a) contour lines of equal peak ground acceleration (PGA) and contour lines of equal spectral acceleration (PSA) for natural period b) 0.2 sec, c) 0.6 sec and d) 1.0 sec. Strong ground motion parameters values are given in g

A similar distribution with the one shown in Fig. 4.5.1.6 is observed for the spectral acceleration at the period of 0.2 sec (Fig. 4.5.1.7.a), whose values are also controlled by higher frequency motions. However, PSA values at larger periods (Fig. 4.5.1.7.b, c) appear to be more controlled by site effects. In the northwest part of the city (municipalities of Efkarpia, Evosmos, Eleftherio Kordelio, Stavroupoli), where site conditions are relatively uniform (Site Class C), strong ground motion diminishes from east to west as the epicentral distance increases. On the contrary, within the central and southeast parts of Thessaloniki, where surface geology gradually changes from rock (to the northeast) to soft soil (to the southwest), strong ground motion diminishes within the "Site Class B" areas and then abruptly increases as it reaches areas covered by stiff or soft soil.

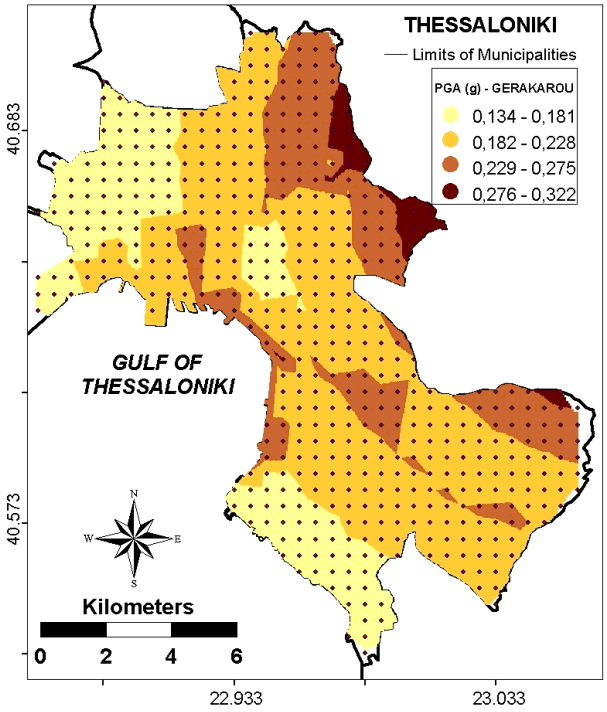

Fig. 4.5.1.6. Peak ground acceleration map (values in g) for the scenario earthquake of M_w=6.2 at the western extension of the 1978 Stivos earthquake rupture zone (Gerakarou – Exohi segment). Dots correspond to the knots of the simulation grid

Taking into account that the periods of 0.2 and 0.6 sec are close to the average resonance periods of typical building constructions in the city of Thessaloniki (0.2 sec for low buildings and 0.6 sec for 6 to 9 storey buildings), we can draw the following conclusions about the impact of the scenario earthquake on the built environment of the city:

- **High-frequency strong ground motion would be more severe along the eastern municipalities (Efkarpia, Pefka, eastern parts of Pylea and Panorama) and in the southern part of the municipality of Thessaloniki, i.e. damage to low constructions would be more likely to occur within these areas.**
- **Levels of low-frequency strong ground motion would be higher in the municipalities of Efkarpia and Polichni (combined source directivity and site effects), the central parts of Pylea and Panorama and the entire municipality of Thessaloniki (site effect). Therefore high constructions within these areas would be more exposed to strong ground shaking and subsequently more prone to damage.**

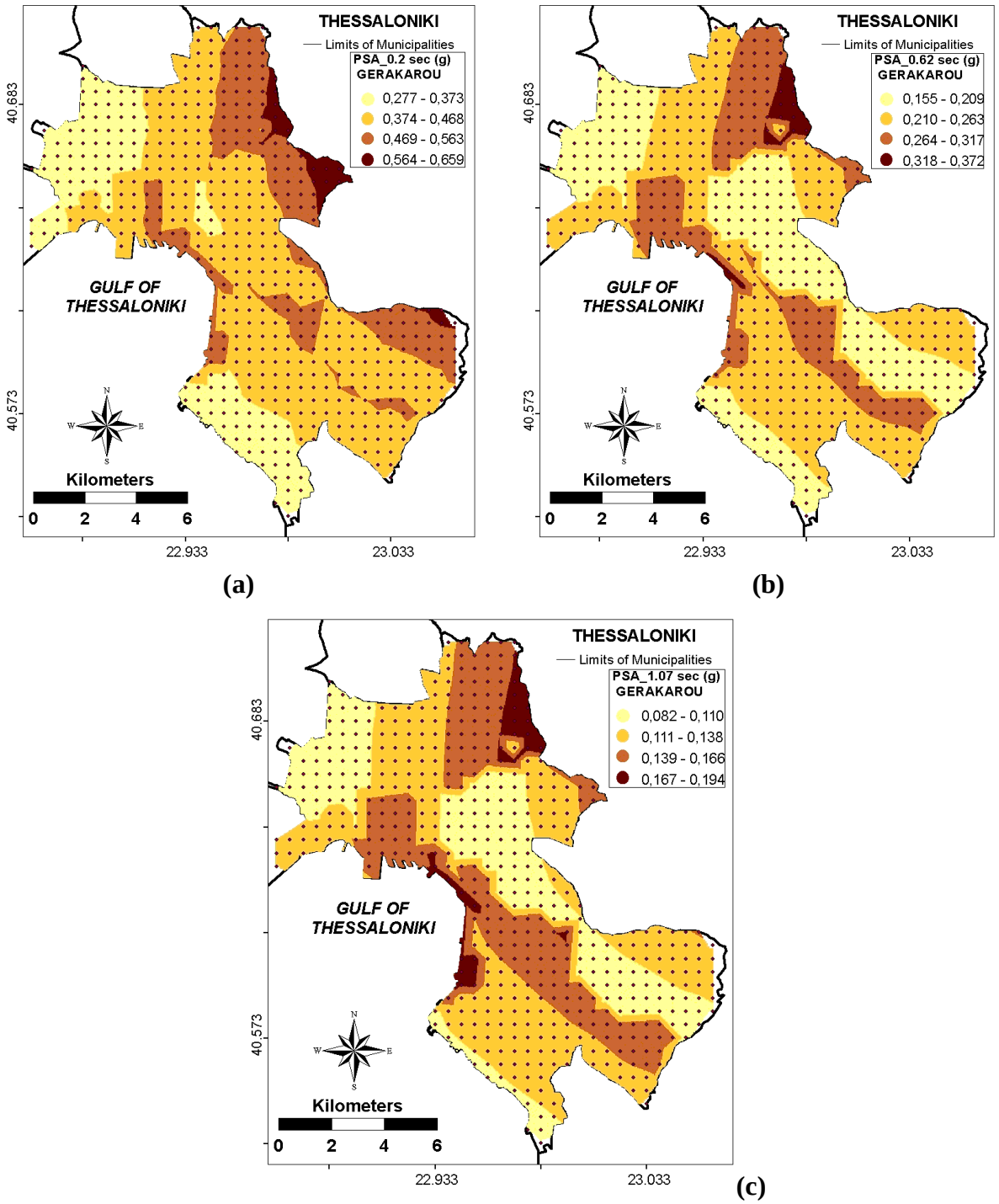

Fig. 4.5.1.7. Spectral acceleration maps (values in g) for the scenario earthquake of M_w=6.2 at the Gerakarou – Exohi fault. Peak spectral acceleration values are shown for three different periods: a) T=0.2 sec, b) T=0.6 sec and c) T=1.0sec. Dots correspond to the knots of the simulation grid

4.5.1.5. Conclusions – discussion

The stochastic method for simulating strong shaking from finite earthquake sources was applied for producing synthetic ground motion maps for a scenario earthquake of M_w=6.2 close to the metropolitan city of Thessaloniki in Northern Greece. The hypothetical earthquake source is considered the western continuation of the 1978 Stivos earthquake fault zone, which according to recent studies (Tranos et al., 2003) is placed in a stress-enhanced area, after the redistribution of stresses caused by the 1978 event, and therefore could rupture in the future.

Distribution of synthetic high-frequency strong ground motion parameters (PGA and PSA at 0.2 sec) show an overall decrease from east to west, as hypocentral distance increases, with the exception of the central coastal part of Thessaloniki, where increased values are attributed to the presence of soft surface geological formations. PGA values vary from ~0.32g in the eastern precinct of Thessaloniki to ~0.13g in its westernmost part. PSA values at 0.2 sec show a similar territorial distribution, ranging from ~0.66g to ~0.28g.

Synthetic PSA maps at 0.6 and 1.0 sec carry the imprint of the site effects as the attenuation of strong ground motion within the "Site Class B" areas, in eastern Thessaloniki, is abruptly interrupted in the transition area to site class C and D surface geology. This means that high buildings (whose resonance lies close to these low-frequency motions) in the municipality of Thessaloniki and in the central part of Pylea and Panorama would experience similar levels of strong shaking with those in the closest to the hypothetical seismic source municipalities (Efkarpia and Evosmos).

Our results can be directly compared with the synthetic strong ground motion maps computed by Theodulidis et al. (2005) for the 1978 Stivos earthquake, as the same method and propagation model have been used in both studies. Therefore, we performed a point-by-point comparison of synthetic PGA values from the 1978 earthquake and from our scenario and computed a mean increase in the level of strong ground motion by a factor of approximately 1.3 for the latter case. This means that although the 1978 earthquake was larger in magnitude, the realization of our scenario earthquake would most probably have larger impact for the city of Thessaloniki.

4.5.1.6. Acknowledgements

We acknowledge financial support from the General Secretariat of Research and Technology (Ministry of Development) of Greece. Z.R and C.B acknowledge financial support from the Ministry of National Education and Religious Affairs of Greece, and from the State Scholarships Foundation (I.K.Y.) of Greece. The authors are grateful to V. Grigoriadis for his help on the preparation of the GIS input files for the production of Figs 4.5.1.6. and 4.5.1.7. Most of the figures were produced by the GMT software (Wessel, Smith, 1998).

4.5.1.7. References

Anastasiadis, A., Raptakis, D. and K. Pitilakis, 2001. Thessaloniki's Detailed Microzoning: Subsurface Structure as basis for Site Response Analysis, PAGEOPH 158(12), 2597 - 2633.

Beresnev, I. A. and G. M. Atkinson, 1997. Modelling finite-fault radiation from the ω^n spectrum, Bull. Seism. Soc. Am. 87, 67 – 84.

Beresnev, I. A. and G. M. Atkinson, 1998. FINSIM – a FORTRAN program for simulating stochastic acceleration time histories from finite faults, Seism. Res. Lett. 69, 27 – 32.

Beresnev, I. A. and G. M. Atkinson, 1999. Generic finite-fault model for ground-motion prediction in eastern North America, Bull. Seism. Soc. Am. 89, 608 – 625.

Beresnev, I. and G. Atkinson, 2001a. Subevent structure of large earthquakes – A ground motion perspective, Geophys. Res. Lett. 28, 53 – 56.

Beresnev, I. and G. Atkinson, 2001b. Correction to "Subevent structure of large earthquakes – A ground motion perspective", Geophys. Res. Lett. 28, 4663.

Beresnev, I. A., and G. M. Atkinson, 2002. Source parameters of earthquakes in eastern and western North America based on finite-fault modeling, Bull. Seism. Soc. Am. 92, 695-710.

Boore, D. M., 1983. Stochastic simulation of high-frequency ground motions based on seismological models of the radiated spectra, Bull. Seism. Soc. Am. 73, 1865 – 1894.

Boore, D. M., 2003. Simulation of ground motion using the stochastic method, Pure Appl. Geophys. 160, 635 – 676.

Castro, R. R., Rovelli, A., Cocco, M., Di Bona, M., and F. Pacor, 2001. Stochastic simulation of strong-motion records from the 26 September 1997 (M_w 6), Umbria-Marche (Central Italy) earthquake, Bull. Seism. Soc. Am. 91, 27-39.

Hanks, T. C., 1979. b values and $\omega^{-\gamma}$ seismic source models: Implications for tectonic stress variations along active crustal fault zones and the estimation of high-frequency strong ground motion, J. Geophys. Res. 84, 2235 – 2242.

Hanks, T. C. and R. K. McGuire, 1981. The character of high-frequency strong ground motion, Bull. Seism. Soc. Am. 71, 2071 – 2095.

Hartzell, S., Harmsen, S., Frankel, A., S. Larsen, 1999. Calculation of broadband time histories of ground motion: comparison of methods and validation using strong-ground motion from the 1994 Northridge earthquake, Bull. Seism. Soc. Am. 89, 1484-1504.

Hatzidimitriou, P. M., 1993. Attenuation of coda waves in Northern Greece, Pure and Appl. Geophys. 140, 63 – 78.

Hatzidimitriou, P. M., 1995. S-wave attenuation in the crust in Northern Greece, Bull. Seism. Soc. Am. 85, 1381 – 1387.

Hough, S. E., Martin, S., Bilham, R., and G. M. Atkinson, 2002. The January 26, 2001 M7.6 Bhuj, India earthquake: Observed and predicted ground motions, Bull. Seism. Soc. Am. 92(6), 2061 - 2079.

Kanamori, H. and D. L. Anderson, 1975. Theoretical basis of some empirical relations in seismology, Bull. Seism. Soc. Am. 65, 1073 – 1095.

Kiratzi, A., 2002. Stress tensor inversions along the westernmost North Anatolian Fault Zone and its continuation into the North Aegean Sea. Geophysical Journal International, 151, 360-376.

Margaris, B. N., B. C. Papazachos, 1994. Seismic Hazard Simulation of Strong Motion Based on Source Parameters in the Area of Greece, Proc. XXIV Gen. Ass. ESC, Sept. 19–24, 1994, Athens, III, 1389 – 1397.

Margaris, B. N., D. M. Boore, 1998. Determination of $\Delta\sigma$ and κ_0 from response spectra of large earthquakes in Greece, Bull. Seism. Soc. Am. 88, 170 – 182.

McGuire, R. K., T. C. Hanks, 1980. Rms accelerations and spectral amplitudes of strong ground motion during the San Fernando, California, earthquake, Bull. Seism. Soc. Am. 70, 1907 – 1919.

Mercier, J.-L., Carey-Gailhardis E., Mouyaris N., Simeakis K., Roundoyanis T. and C. Anghelidis, 1983. Structural analysis of recent and active faults and regional state of stress in the epicentral area of the 1978 Thessaloniki earthquakes (Northern Greece), Tectonics 2, 577 – 600.

NEHRP recommended provisions for seismic regulations for new buildings, 1994, Federal Emergency Management Agency (FEMA), Washington, D.C.

Papastamatiou, D., Margaris, V., N. Theodoulidis, 1993. Estimation of the parameters controlling strong ground motion from shallow earthquakes in Greece, Proc. 2nd Hell. Geoph. Congr., May 5–7, 1993, Florina, I, 192 – 201.

Papazachos B. C., C. Papazachou, 2003. The earthquakes of Greece. Ziti Publ. Co., Thessaloniki, Greece, 286 pp (in Greek).

Papazachos, B., Mountrakis, D., Psilovikos, A., G. Leventakis, 1979. Surface fault traces and fault plane solutions of the May-June 1978 shocks in the Thessaloniki area, North Greece, Tectonophysics 53, 171 – 183.

Papazachos, B, Scordilis, E., Panagiotopoulos, D., Papazachos, C., G. Karakaisis, 2004. Global relations between seismic fault parameters and earthquakes moment, Bull. Geol. Soc. Greece, 36, 1482 – 1489.

Pavlides, S., A. Kilias, 1987. Neotectonic and active faults along the Serbomacedonian zone (SE Chalkidiki, Northern Greece), Ann. Tectonicae 1, 97 – 104.

Roumelioti, Z., A. Kiratzi, 2002. Stochastic simulation of strong-motion records from the 15 April 1979 (M 7.1) Montenegro earthquake, Bull. Seism. Soc. Am. 92, 1095-1101.

Roumelioti, Z., Kiratzi, A., Theodoulidis, N., Ch. Papaioannou, 2000. A comparative study of a stochastic and deterministic simulation of strong ground motion applied to the Kozani-Grevena (NW Greece) 1995 sequence, Annali di Geofisica, 43, 951 – 966.

Roumelioti, Z., Kiratzi, A., Theodoulidis, N., Kalogeras, I., G. Stavrakakis, 2003. Rupture directivity during the September 7, 1999 (M_w 5.9) Athens (Greece) earthquake obtained from strong-motion records, Pure and Appl. Geophys., 160 (12), 2301 - 2318.

Roumelioti, Z., Kiratzi, A., N. Theodoulidis, 2004. Stochastic strong ground motion simulation of the 7 September 1999 Athens (Greece) earthquake, Bull. Seism. Soc. Am, 94(3), 1036 - 1052.

Roumelioti, Z., Theodulidis, N.,A. Kiratzi, 2005. Slip distribution and forward modeling of geodetic and seismological observations of the 20 June 1978 Thessaloniki (Northern Greece) earthquake, submitted.

Soufleris, C., G. Stewart, 1981. A source study of the Thessaloniki (northern Greece) 1978 earthquake sequence, Geophys. J. R. astr. Soc. 67, 343 – 358.

Stiros, S. C., A. Drakos, 2000. Geodetic constraints on the fault pattern of the 1978 Thessaloniki (Northern Greece) earthquake (M_S=6.4), Geophys. J. Int. 143, 679 – 688.

Theodulidis, N., Roumelioti, Z., Panou, A., Savvaidis, A., Kiratzi, A., Grigoriadis, V., Dimitriou, P., T. Chatzigogos, 2005. Retrospective prediction of macroseismic intensities using strong ground motion simulation: the case of the 1978 Thessaloniki (Greece) earthquake (M6.5), submitted for publication.

Tranos, M. D., Papadimitriou, E. E., A. A. Kilias, 2003. Thessaloniki – Gerakarou Fault Zone (TGFZ): the western extension of the 1978 Thessaloniki earthquake fault (Northern Greece) and seismic hazard assessment, J. Struct. Geol., 25(12), 2109 – 2123.

Wells, D. L., K. J. Coppersmith, 1994. New empirical relationships among magnitude, rupture length, rupture width, rupture area and surface displacement, Bull. Seism. Soc. Am. 84, 974-1002.

Wessel, P., W. H. F. Smith, 1998. New improved version of the Generic Mapping Tools released, EOS Trans. AGU 79, 579.